2023 American Control Conference (ACC)
San Diego, CA, USA. May 31 - June 2, 2023

Predictive Cost Adaptive Control for Harmonic Disturbance Rejection in Systems with Underdamped, Undermodeled, and Undersampled Dynamics

Riley J. Richards, Nima Mohseni, S. A. U. Islam, and Dennis S. Bernstein

Abstract— **Lightly damped modes that lie within or outside the controller bandwidth of an attitude control system are challenging. As an active control strategy for harmonic disturbances, the present paper applies predictive cost adaptive control (PCAC) to a system with a rigid-body mode and a lightly damped mode that is unmodeled and possibly aliased. PCAC is applied to the specific case of resonance, where the frequency of the exogenous harmonic disturbance coincides with the peak-amplification frequency of the system. LQG control with and without an internal model and with known and uncertain modal frequency provides a baseline for comparison with PCAC, which uses online identification and requires no prior knowledge of the system dynamics or disturbance spectrum. The numerical comparison accounts for the intersample behavior of the lightly damped mode.**

I. Introduction

Lightly damped modes that lie within or outside the controller bandwidth of an attitude control system are challenging. These modes may be excited by either the command or the disturbance, especially when the disturbance is a harmonic signal whose frequency coincides with a peak-amplification frequency of the system; this is the case of resonance. In practice, input shaping [1] and loop shaping (gain and phase stabilization) [2] can be used to avoid excitation of these modes by the attitude control system, and passive, semi-active, or active control techniques can be used to improve settling time [3]–[5]. If the disturbance is measured, then feedforward techniques can be used [6]; however, the present paper focuses on feedback control.

When active control methods are used, a system and disturbance model may be needed. The standard approach to this problem is to apply LQG control with frequency shaping of the cost in order to account for the lightly damped mode and disturbance [7], [8]. A related approach is to embed an internal model in the loop as part of the controller, thereby cancelling the effect of the disturbance [9], [10]; integral control for step-command following and step-disturbance rejection is a special case of this technique.

The present paper focuses on active control of systems with lightly damped modes that are either poorly modeled or unmodeled. The lack of an accurate model may be due to the inability to perform system identification, or it may arise from unmodelable or nonrepeatable effects due to the environment. In this case, frequency shaping and internal model control may result in a detuned controller with poor performance.

Riley J. Richards, Nima Mohseni, S. A. U. Islam, and Dennis S. Bernstein are with the Department of Aerospace Engineering, University of Michigan, Ann Arbor, MI 48109.

In order to account for model uncertainty, robust control methods such as gain and phase stabilization can be used. Alternatively, adaptive controllers that can learn and adjust their gains to the actual system dynamics and disturbance are of interest. Within the context of direct adaptive control, however, unmodeled lightly damped modes may lead to divergence [11].

The present paper addresses the problem of suppressing the vibrations of a lightly damped mode by applying predictive cost adaptive control (PCAC) [12]. PCAC is a variation of model predictive control (MPC), which has been extensively developed [13], [14] and applied to vibration control [15]. In particular, PCAC uses online system identification to obtain a model of the system, and takes advantage of a system realization that facilitates output (partial-state) feedback. Since MPC is based on optimization over a future horizon and since vibration suppression entails disturbance rejection, a critical issue concerns the ability of PCAC to correctly predict the response to the future, unknown disturbance. This issue was addressed in [16], where it was shown that system identification in the presence of harmonic disturbances is able to build a model that correctly forecasts not only the frequency of the future response but also its amplitude and phase. This property is essential to the application of PCAC to systems that are subjected to harmonic disturbances.

PCAC was applied to vibration suppression in [17], [18]. The present paper goes beyond these works in two ways. First, we consider the case where the system dynamics include a rigid body mode, which is often the case in practice. This problem is an extension of the benchmark problem in [19], where, in the present paper, the setting is sampled-data control, the dynamics of the lightly damped mode are uncertain, and the disturbance is harmonic at the peak-amplification frequency. Second, we consider the case where the unmodeled lightly damped mode may lie either within or outside the controller bandwidth. In the latter case, aliasing may occur, and one of the goals of this paper is to determine how severe undersampling (or, equivalently, high-frequency unmodeled dynamics) affects the performance of PCAC. As a baseline comparison, we apply LQG to the same problem assuming that the peak-amplification frequency of the lightly damped mode is uncertain.

The contents of the paper are as follows. Section II formulates the sampled-data control problem; Section III reviews discrete-time LQG control with an internal model; Section IV reviews PCAC; and Section V compares LQG with PCAC.

II. Harmonic Disturbance Rejection under Sampled-Data Control

We consider the sampled-data control architecture shown in Figure 1. The continuous-time system G is represented as a state-space model, which is discretized according to sample-and-hold operations. In particular, G is represented by

$$\dot{x}(t) = A_{\rm CT}x(t) + B_{\rm CT}u(t) + D_{1,\rm CT}w(t), \quad (1)$$
$$y(t) = C_{\rm CT}x(t) + D_{2,\rm CT}v(t), \quad (2)$$

where $x(t) \in \mathbb{R}^n$ is the state, $w(t) \in \mathbb{R}^{l_w}$ is the disturbance, $y(t) \in \mathbb{R}^p$ is the measurement, $v(t) \in \mathbb{R}^{l_v}$ is the sensor noise, $A_{\rm CT} \in \mathbb{R}^{n\times n}$, $B_{\rm CT} \in \mathbb{R}^{n\times m}$, $C_{\rm CT} \in \mathbb{R}^{p\times n}$, $D_{1,\rm CT} \in \mathbb{R}^{n\times l_w}$, and $D_{2,\rm CT} \in \mathbb{R}^{p\times l_v}$. The disturbance $w(t)$ is matched if there exists $\overline{U} \in \mathbb{R}^{m\times m}$ such that $D_1 = B\overline{U}$; otherwise, the disturbance is unmatched. Note that, if $B = D_1$, then the disturbance is matched and $\overline{U} = I$. The control input $u(t)$ is piecewise constant within each interval $[kT_{\rm s}, (k+1)T_{\rm s})$, at the value u_k, where $T_{\rm s} > 0$ is the sample interval whose units are sec/step and $k = 1, 2, \ldots$ denotes the step. The output $y(t)$ of G is corrupted by sensor noise $v(t)$. The sampling operation yields $y_k \triangleq y(kT_{\rm s}) + v_k$, where $v_k \triangleq v(kT_{\rm s}) \in \mathbb{R}^p$ is the sampled sensor noise.

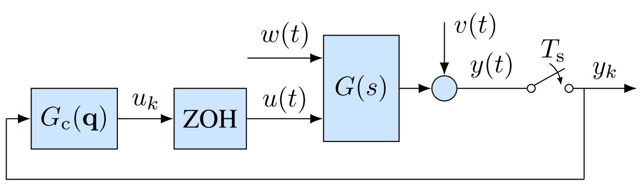

Fig. 1: Disturbance rejection under sampled-data control. The objective is to reject the disturbance $w(t)$. The sample interval, whose units are sec/step, is denoted by $T_{\rm s}$, and ZOH denotes zero-order hold. All sample-and-hold operations are synchronous.

The continuous-time system (1), (2) with sample-and-hold operations is discretized as

$$x_{k+1} = Ax_k + Bu_k + D_1w_k, \quad (3)$$
$$y_k = Cx_k + D_2v_k, \quad (4)$$

where $x_k \triangleq x(kT_{\rm s})$, $y_k \triangleq y(kT_{\rm s})$, and A, B, D_1, C, and D_2 are the discretized versions of $A_{\rm CT}, B_{\rm CT}, D_{1,\rm CT}, C_{\rm CT}$, and $D_{2,\rm CT}$, respectively. Define the discrete-time disturbance and sensor-noise covariances $V_1 \triangleq D_1D_1^{\rm T}$ and $V_2 \triangleq D_2D_2^{\rm T}$.

In later sections, the controller $G_{\rm c}(\mathbf{q})$ will be either a discrete-time LQG controller, with or without an internal model, or an adaptive control based on MPC. The performance of all controllers will be evaluated in terms of the root-mean-square (RMS) value of $y(t)$. This measure includes the intersample behavior of $y(t)$, that is, the values of $y(t)$ within each sample interval as determined by numerical integration using an integration step size that is much smaller than the sample interval $T_{\rm s}$.

III. Sampled-Data LQG Control

Consider the discrete-time dynamical system (3), (4) where w_k and v_k are uncorrelated standard Gaussian white-noise processes. The goal is to find a controller that minimizes the cost

$$J(A_{\rm c}, B_{\rm c}, C_{\rm c}) \triangleq \lim_{k\to\infty} \mathbb{E}(x_k^{\rm T}R_1x_k + u_k^{\rm T}R_2u_k), \quad (5)$$

where $\mathbb{E}$ denotes expected value. The optimal controller is given by [20]

$$\hat{x}_{k+1} = (A - BK - LC)\hat{x}_k + Ly_k, \quad (6)$$
$$u_k = -K\hat{x}_k, \quad (7)$$

where L is the Kalman gain

$$L \triangleq AQC^{\rm T}(CQC^{\rm T} + V_2)^{-1}, \quad (8)$$

Q is the solution of the observer Riccati equation

$$Q = AQA^{\rm T} - AQC^{\rm T}(CQC^{\rm T} + V_2)^{-1}CQA^{\rm T} + V_1, \quad (9)$$

K is the feedback gain

$$K \triangleq (B^{\rm T}PB + R_2)^{-1}B^{\rm T}PA, \quad (10)$$

and P is the solution of the regulator Riccati equation

$$P = A^{\rm T}PA - A^{\rm T}PB(B^{\rm T}PB + R_2)^{-1}B^{\rm T}PA + R_1. \quad (11)$$

Although LQG is based on the assumption that w_k is white noise, this paper focuses on the case where w_k is harmonic. In this case, LQG can be used to obtain a stabilizing controller that includes a suitable internal model [9], [10]. This can be done by cascading an internal model of the disturbance with the plant dynamics and then synthesizing an LQG controller for the augmented dynamics. For an internal model with order $n_{\rm im}$, this procedure, which is shown in Figure 2, leads to a controller of order $n + 2n_{\rm im}$.

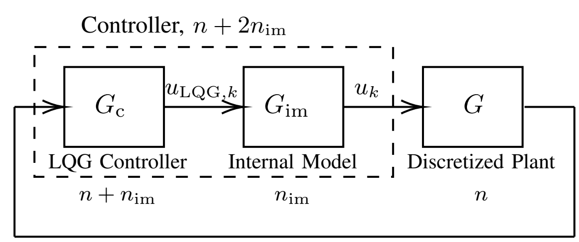

Fig. 2: Block diagram of the LQG internal model control approach. The internal model $G_{\rm im}$ is embedded in the loop, and an LQG controller of order $n + n_{\rm im}$ is synthesized for the cascaded system. The implemented controller, which consists of the LQG controller and the internal model, thus has order $n + 2n_{\rm im}$.

To illustrate this procedure for the case of a single harmonic, the dynamics of the internal model are given by

$$x_{\rm im,k+1} = A_{\rm im}x_{\rm im,k} + B_{\rm im}u_{{\rm LQG},k}, \ u_k = C_{\rm im}x_{{\rm im},k}, \quad (12)$$

$$A_{\rm im} \triangleq \begin{bmatrix} \cos(\omega_{\rm dis}T_{\rm s}) & \frac{1}{\omega_{\rm dis}}\sin(\omega_{\rm dis}T_{\rm s}) \\ -\omega_{\rm dis}\sin(\omega_{\rm dis}T_{\rm s}) & \cos(\omega_{\rm dis}T_{\rm s}) \end{bmatrix}, \quad (13)$$

$$B_{\rm im} \triangleq \begin{bmatrix} \frac{-1}{\omega_{\rm dis}^2}(\cos(\omega_{\rm dis}T_{\rm s}) - 1) \\ \frac{1}{\omega_{\rm dis}}\sin(\omega_{\rm dis}T_{\rm s}) \end{bmatrix} \quad (14)$$

$$C_{\rm im} \triangleq \begin{bmatrix} 1 & 0 \end{bmatrix}, \quad (15)$$

where the eigenvalues of $A_{\rm im}$ correspond to the spectrum of the harmonic disturbance at the disturbance frequency $\omega_{\rm dis}$. The augmented dynamics that LQG uses to create the controller are thus given by

$$\hat{x}_{\mathrm{aug},k} \triangleq \begin{bmatrix} \hat{x}_k \\ \hat{x}_{\mathrm{im},k} \end{bmatrix}, \ A_{\mathrm{aug}} \triangleq \begin{bmatrix} A & BC_{\mathrm{im}} \\ 0 & A_{\mathrm{im}} \end{bmatrix}, \tag{16}$$

$$B_{\mathrm{aug}} \triangleq \begin{bmatrix} 0 \\ B_{\mathrm{im}} \end{bmatrix}, \ C_{\mathrm{aug}} \triangleq \begin{bmatrix} C & 0 \end{bmatrix}, \tag{17}$$

where $\hat{x}_{\mathrm{im},k}$ is the estimated state of the internal model. The resulting observer and controller gains and the associated Riccati equations are given by

$$L = A_{\mathrm{aug}} Q C_{\mathrm{aug}}^{\mathrm{T}} (C_{\mathrm{aug}} Q C_{\mathrm{aug}}^{\mathrm{T}} + V_2)^{-1}, \tag{18}$$

$$Q = A_{\mathrm{aug}} Q A_{\mathrm{aug}}^{\mathrm{T}} - A_{\mathrm{aug}} Q C^{\mathrm{T}} (C_{\mathrm{aug}} Q C_{\mathrm{aug}}^{\mathrm{T}} + V_2)^{-1} C_{\mathrm{aug}} Q A_{\mathrm{aug}}^{\mathrm{T}} + V_1, \tag{19}$$

$$K = (B_{\mathrm{aug}}^{\mathrm{T}} P B_{\mathrm{aug}} + R_2)^{-1} B_{\mathrm{aug}}^{\mathrm{T}} P A_{\mathrm{aug}}, \tag{20}$$

$$P = A_{\mathrm{aug}}^{\mathrm{T}} P A_{\mathrm{aug}} - A_{\mathrm{aug}}^{\mathrm{T}} P B_{\mathrm{aug}} (B_{\mathrm{aug}}^{\mathrm{T}} P B_{\mathrm{aug}} + R_2)^{-1} B_{\mathrm{aug}}^{\mathrm{T}} P A_{\mathrm{aug}} + R_1. \tag{21}$$

The resulting controller of order $n + 2n_{\mathrm{im}}$ has the form

$$\begin{bmatrix} \hat{x}_{\mathrm{aug},k+1} \\ x_{\mathrm{im,k+1}} \end{bmatrix} = \begin{bmatrix} A_{\mathrm{aug}} - B_{\mathrm{aug}} K - L C_{\mathrm{aug}} & 0 \\ -B_{\mathrm{im}} K & A_{\mathrm{im}} \end{bmatrix} \begin{bmatrix} \hat{x}_{\mathrm{aug},k} \\ x_{\mathrm{im,k}} \end{bmatrix} + \begin{bmatrix} L \\ 0 \end{bmatrix} y_k, \tag{22}$$

$$u_k = \begin{bmatrix} 0 & C_{\mathrm{im}} \end{bmatrix} \begin{bmatrix} \hat{x}_{\mathrm{aug},k} \\ x_{\mathrm{im,k}} \end{bmatrix}. \tag{23}$$

The procedure for using LQG to construct a stabilizing controller with an internal model of the harmonic disturbance assumes that the frequency ω_{dist} is known. In this case, the resulting controller has high gain at ω_{dist}, and thus the closed-loop transfer function from w to y has a notch, thereby rejecting the disturbance.

IV. Predictive Cost Adaptive Control

PCAC combines online identification with output-feedback MPC.

A. Online Identification

Consider the MIMO input-output model

$$\hat{y}_k = -\sum_{i=1}^{\hat{n}} \hat{F}_i y_{k-i} + \sum_{i=1}^{\hat{n}} \hat{G}_i u_{k-i}, \tag{24}$$

where $k \geq 0$ is the step, $\hat{n} \geq 1$ is the identification data window, $\hat{F}_k \in \mathbb{R}^{p \times p}$ and $\hat{G}_k \in \mathbb{R}^{p \times m}$ are the estimated model coefficients, and $u_k \in \mathbb{R}^m$, $y_k \in \mathbb{R}^p$, and $\hat{y}_k \in \mathbb{R}^p$ are the inputs, outputs and predicted outputs.

To estimate the coefficients $\hat{F}_k$ and $\hat{G}_k$ online, we use recursive least squares (RLS) with variable-rate forgetting [21], which minimizes the cumulative cost

$$J_k(\hat{\theta}) = \sum_{i=0}^{k} \frac{\rho_i}{\rho_k} z_i^{\mathrm{T}}(\hat{\theta}) z_i(\hat{\theta}) + \frac{1}{\rho_k} (\hat{\theta} - \theta_0)^{\mathrm{T}} P_0^{-1} (\hat{\theta} - \theta_0), \tag{25}$$

where $\rho_k \triangleq \prod_{j=0}^{k} \lambda_j^{-1} \in \mathbb{R}$, $\lambda_k \in (0, 1]$ is the forgetting factor, $P_0 \in \mathbb{R}^{[\hat{n}p(m+p)] \times [\hat{n}p(m+p)]}$ is positive definite, $\theta_0 \in \mathbb{R}^{[\hat{n}p(m+p)]}$ is the initial estimate of the coefficient vector, and the performance variable $z_i(\hat{\theta}) \in \mathbb{R}^p$ is defined as

$$z_k(\hat{\theta}) \triangleq y_k + \sum_{i=1}^{\hat{n}} \hat{F}_i y_{k-i} - \sum_{i=1}^{\hat{n}} \hat{G}_i u_{k-i}, \tag{26}$$

where the vector $\hat{\theta} \in \mathbb{R}^{[\hat{n}p(m+p)]}$ of coefficients to be estimated is defined by

$$\hat{\theta} \triangleq \mathrm{vec} \begin{bmatrix} \hat{F}_1 & \cdots & \hat{F}_{\hat{n}} & \hat{G}_1 & \cdots & \hat{G}_{\hat{n}} \end{bmatrix}. \tag{27}$$

Defining the regressor matrix $\phi_k \in \mathbb{R}^{p \times [\hat{n}p(m+p)]}$ by

$$\phi_k \triangleq \begin{bmatrix} -y_{k-1}^{\mathrm{T}} & \cdots & -y_{k-\hat{n}}^{\mathrm{T}} & u_{k-1}^{\mathrm{T}} & \cdots & u_{k-\hat{n}}^{\mathrm{T}} \end{bmatrix} \otimes I_p, \tag{28}$$

the performance variable can then be written as

$$z_k(\hat{\theta}) = y_k - \phi_k \hat{\theta}. \tag{29}$$

The global minimizer $\theta_{k+1} \triangleq \mathrm{argmin}_{\hat{\theta}} J_k(\hat{\theta})$ is computed by RLS as

$$L_k = \lambda_k^{-1} P_k \tag{30}$$

$$P_{k+1} = L_k - L_k \phi_k^{\mathrm{T}} (I_p + \phi_k L_k \phi_k^{\mathrm{T}})^{-1} \phi_k L_k \tag{31}$$

$$\theta_{k+1} = \theta_k + P_{k+1} \phi_k^{\mathrm{T}} (y_k - \phi_k \theta_k), \tag{32}$$

where

$$\theta_{k+1} = \mathrm{vec} \begin{bmatrix} \hat{F}_{1,k+1} & \cdots & \hat{F}_{\hat{n},k+1} & \hat{G}_{1,k+1} & \cdots & \hat{G}_{\hat{n},k+1} \end{bmatrix}. \tag{33}$$

The variable-rate forgetting (VRF) factor λ_k is developed in [22] and given by

$$\lambda_k = \frac{1}{1 + \eta g(z_{k-\tau_{\mathrm{d}}}, \ldots, z_k) \mathbf{1}[g(z_{k-\tau_{\mathrm{d}}}, \ldots, z_k)]} \tag{34}$$

where $\mathbf{1} : \mathbb{R} \to \{0, 1\}$ is the unit step function, and

$$g(z_{k-\tau_{\mathrm{d}}}, \ldots, z_k) \triangleq \sqrt{\frac{\tau_{\mathrm{n}}}{\tau_{\mathrm{d}}} \frac{(\Sigma_{\tau_{\mathrm{n}}}(z_{k-\tau_{\mathrm{n}}}, \ldots, z_k) \Sigma_{\tau_{\mathrm{d}}}(z_{k-\tau_{\mathrm{d}}}, \ldots, z_k)^{-1})}{c}} - \sqrt{f}, \tag{35}$$

where $\eta > 0$ and $p \leq \tau_{\mathrm{n}} < \tau_{\mathrm{d}}$ represent numerator and denominator window lengths, respectively. In (35), $\Sigma_{\tau_{\mathrm{n}}}$ and $\Sigma_{\tau_{\mathrm{d}}} \in \mathbb{R}^{p \times p}$ are the sample variances of the respective window lengths, c is a constant given by

$$a \triangleq \frac{(\tau_{\mathrm{n}} + \tau_{\mathrm{d}} - p - 1)(\tau_{\mathrm{d}} - 1)}{(\tau_{\mathrm{d}} - p - 3)(\tau_{\mathrm{d}} - p)}, \ b \triangleq 4 + \frac{(p\tau_{\mathrm{n}} + 2)}{(a - 1)}, \quad c \triangleq \frac{p\tau_{\mathrm{n}}(b - 2)}{b(\tau_{\mathrm{d}} - p - 1)}, \tag{36}$$

$f \triangleq F_{p\tau_{\mathrm{n}}, b}^{-1}(1 - \alpha)$ is a thresholding constant, where $F_{p\tau_{\mathrm{n}}, b}^{-1}(x)$ is the inverse cumulative distribution function of the F-distribution with degrees of freedom $p\tau_{\mathrm{n}}$ and b, and α is the significance level [23]. By choosing $\tau_{\mathrm{d}} >> \tau_{\mathrm{n}}$, $\Sigma_{\tau_{\mathrm{d}}}$ approximates the long-term variance of z_k while $\Sigma_{\tau_{\mathrm{n}}}$ approximates the short-term variance of z_k. Therefore, when $g(z_{k-\tau_d}, \ldots, z_k) > 0$, the short-term variance is statistically larger than the long-term variance. In particular, (34) suspends forgetting when the short-term variance is statistically smaller than the long-term variance, preventing forgetting in RLS due to sensor noise, and enabling forgetting when the magnitude of the identification error increases.

For receding-horizon control, the input-output model (24) is written as the block observable canonical form state-space realization

$$x_{1|k} \triangleq \hat{A}_k \hat{x}_k + \hat{B}_k u_k, \tag{37}$$

$$y_k = \hat{C}\hat{x}_k, \tag{38}$$

where $x_{1|k} \in \mathbb{R}^{\hat{n}p}$ is the one-step predicted state, $\hat{x}_k \triangleq \begin{bmatrix}\hat{x}_{1,k}^{\mathrm{T}} & \cdots & \hat{x}_{\hat{n},k}^{\mathrm{T}}\end{bmatrix}^{\mathrm{T}} \in \mathbb{R}^{\hat{n}p}$ is the state estimate, and

$$\hat{x}_{1,k} \triangleq y_k, \tag{39}$$

$$\hat{x}_{i,k} \triangleq -\sum_{j=1}^{\hat{n}-i+1} \hat{F}_{i+j-1,k+1} y_{k-j} + \sum_{j=1}^{\hat{n}-i+1} \hat{G}_{i+j-1,k+1} u_{k-j}, \quad i = 2,\ldots,\hat{n} \tag{40}$$

$$\hat{A}_k \triangleq \begin{bmatrix} -\hat{F}_{1,k+1} & I_p & \cdots\cdots & 0_{p\times p} \\ \vdots & 0_{p\times p} & \ddots & \vdots \\ \vdots & \vdots & \ddots\ \ddots & 0_{p\times p} \\ \vdots & \vdots & \ddots & I_p \\ -\hat{F}_{\hat{n},k+1} & 0_{p\times p} & \cdots\cdots & 0_{p\times p} \end{bmatrix}, \hat{B}_k \triangleq \begin{bmatrix} \hat{G}_{1,k+1} \\ \hat{G}_{2,k+1} \\ \vdots \\ \hat{G}_{\hat{n},k+1} \end{bmatrix}, \tag{41}$$

$$\hat{C} \triangleq \begin{bmatrix} I_p & 0_{p\times p} & \cdots & 0_{p\times p} \end{bmatrix}, \tag{42}$$

B. Model Predictive Control

The ℓ-step predicted output of (38) for a sequence of ℓ future controls is given by

$$Y_{1|k,l} = \hat{\Gamma}_{k,\ell} x_{1|k} + \hat{T}_{k,\ell} U_{1|k,\ell}, \tag{43}$$

where

$$Y_{1|k,\ell} \triangleq \begin{bmatrix} y_{1|k} \\ \vdots \\ y_{\ell|k} \end{bmatrix} \in \mathbb{R}^{\ell p}, \quad U_{1|k,\ell} \triangleq \begin{bmatrix} u_{1|k} \\ \vdots \\ u_{\ell|k} \end{bmatrix} \in \mathbb{R}^{\ell m}, \tag{44}$$

and $\hat{\Gamma}_{k,\ell} \in \mathbb{R}^{\ell p \times \hat{n}p}$ and $\hat{T}_{k,\ell} \in \mathbb{R}^{\ell p \times \ell m}$ are

$$\hat{\Gamma}_{k,\ell} \triangleq \begin{bmatrix} \hat{C} \\ \hat{C}\hat{A}_k \\ \vdots \\ \hat{C}\hat{A}_k^{\ell-1} \end{bmatrix}, \tag{45}$$

$$\hat{T}_{k,\ell} \triangleq \begin{bmatrix} 0_{p\times m} & \cdots & \cdots & \cdots & \cdots & \cdots & 0_{p\times m} \\ \hat{H}_{k,1} & 0_{p\times m} & \cdots & \cdots & \cdots & \cdots & 0_{p\times m} \\ \hat{H}_{k,2} & \hat{H}_{k,1} & 0_{p\times m} & \cdots & \cdots & \cdots & 0_{p\times m} \\ \hat{H}_{k,3} & \hat{H}_{k,2} & \hat{H}_{k,1} & 0_{p\times m} & \cdots & \cdots & 0_{p\times m} \\ \hat{H}_{k,4} & \hat{H}_{k,3} & \hat{H}_{k,2} & \ddots & \ddots & & \vdots \\ \vdots & \vdots & \vdots & \ddots & \ddots & \ddots & 0_{p\times m} \\ \hat{H}_{k,\ell-1} & \hat{H}_{k,\ell-2} & \hat{H}_{k,\ell-3} & \cdots & \hat{H}_{k,2} & \hat{H}_{k,1} & 0_{p\times m} \end{bmatrix}, \tag{46}$$

where $\hat{H}_{k,i} \in \mathbb{R}^{p\times m}$ is defined by $\hat{H}_{k,i} \triangleq \hat{C}\hat{A}_k^{i-1}\hat{B}_k$.

Let $\mathcal{R}_{k,\ell} \triangleq \begin{bmatrix} r_{k+1}^{\mathrm{T}} \cdots r_{k+\ell}^{\mathrm{T}} \end{bmatrix}^{\mathrm{T}} \in \mathbb{R}^{\ell p_{\mathrm{t}}}$ be the vector of ℓ future commands, let $Y_{\mathrm{t},1|k,\ell} \triangleq C_{\mathrm{t},\ell} Y_{1|k,\ell}$ be the ℓ-step predicted tracking output, where $C_{\mathrm{t},\ell} \triangleq I_\ell \otimes C_{\mathrm{t}} \in \mathbb{R}^{\ell p_{\mathrm{t}} \times \ell p}$ and $C_{\mathrm{t}} y_{i|k}$ computes the tracking outputs from $y_{i|k}$. Defining

$$\Delta U_{1|k,\ell} \triangleq \begin{bmatrix} u_{1|k} - u_k \\ u_{2|k} - u_{1|k} \\ \vdots \\ u_{\ell|k} - u_{\ell-1|k} \end{bmatrix} \in \mathbb{R}^{\ell m}, \tag{47}$$

the receding horizon optimization problem is then given by

$$\min_{U_{1|k,\ell}} \left(Y_{\mathrm{t},1|k,\ell} - \mathcal{R}_{k,\ell}\right)^{\mathrm{T}} Q \left(Y_{\mathrm{t},1|k,\ell} - \mathcal{R}_{k,\ell}\right) + \Delta U_{1|k,\ell}^{\mathrm{T}} R \Delta U_{1|k,\ell}, \tag{48}$$

subject to

$$U_{\min} \le U_{1|k,\ell} \le U_{\max} \tag{49}$$

$$\Delta U_{\min} \le \Delta U_{1|k,\ell} \le \Delta U_{\max}, \tag{50}$$

where $Q \in \mathbb{R}^{\ell p_{\mathrm{t}} \times \ell p_{\mathrm{t}}}$ is the positive definite tracking weight, $R \in \mathbb{R}^{\ell m \times \ell m}$ is the positive definite control move-size weight, $U_{\min} \triangleq 1_\ell \otimes u_{\min} \in \mathbb{R}^{\ell m}$, $U_{\max} \triangleq 1_\ell \otimes u_{\max} \in \mathbb{R}^{\ell m}$, $\Delta U_{\min} \triangleq 1_\ell \otimes \Delta u_{\min} \in \mathbb{R}^{\ell m}$, and $\Delta U_{\max} \triangleq 1_\ell \otimes \Delta u_{\max} \in \mathbb{R}^{\ell m}$.

In summary, at each time step, online identification is performed to find input-output model coefficients θ_{k+1}, which are then used to create a state space realization $\left(\hat{A}_k, \hat{B}_k, \hat{C}\right)$. The state-space realization is then used in a receding horizon optimization problem to solve for the ℓ-step controls $U_{1|k,\ell}$. The control input for the next step is then given by $u_{1|k}$, and the rest of $U_{1|k,\ell}$ is discarded.

V. Example

Consider the 4th-order system

$$G(s) = \frac{\omega_{\mathrm{n}}^2}{s^2(s^2 + 2\zeta\omega_{\mathrm{n}} s + \omega_{\mathrm{n}}^2)}, \tag{51}$$

which includes a rigid-body mode and a lightly damped mode, where $\omega_{\mathrm{n}} = 2\pi$ rad/sec and $\zeta = 0.01$. To capture resonance, the system is subject to a harmonic disturbance at the peak-amplification frequency $\omega_{\mathrm{p}} = \omega_{\mathrm{n}}\sqrt{1-2\zeta^2}$, that is, $\omega_{\mathrm{dis}} = \omega_{\mathrm{p}}$. Note that ω_{p} is close to, but slightly different from, the damped natural frequency $\omega_{\mathrm{d}} = \omega_{\mathrm{n}}\sqrt{1-\zeta^2}$ [24]. Define the state space realization of (51)

$$A_{\mathrm{CT}} \triangleq \begin{bmatrix} 0 & 1 & 0 & 0 \\ 0 & 0 & 1 & 0 \\ 0 & 0 & 0 & 1 \\ 0 & 0 & -\omega_{\mathrm{n}}^2 & -2\zeta\omega_{\mathrm{n}} \end{bmatrix}, \quad B_{\mathrm{CT}} = D_{1,\mathrm{CT}} \triangleq \begin{bmatrix} 0 \\ 0 \\ 0 \\ \omega_{\mathrm{n}}^2 \end{bmatrix}, \tag{52}$$

$$C_{\mathrm{CT}} \triangleq \begin{bmatrix} 1 & 0 & 0 & 0 \end{bmatrix}, \quad D_{2,\mathrm{CT}} \triangleq 0. \tag{53}$$

In the following subsections we compute the resulting steady-state root-mean-square (RMS) value of the position output obtained from LQG with and without an internal model of the disturbance as well as from PCAC with an uninformative initial model. As shown in Figure 1, the dynamics (52), (53) are discretized with sample interval T_{s}.

A. LQG-based disturbance rejection

Two LQG controllers are considered. In the first case, LQG is applied directly to the 4th-order dynamics. In the second case, the system dynamics are augmented by a 2nd-order internal model, and the LQG controller is synthesized for the augmented 6th-order plant. The final controller consists of the 6th-order LQG controller and the internal model, and thus is 8th order.

In Figure 3(a) and (b), LQG is applied to (51), with and without an internal model, using sampled-data control with two values of $T_{\rm s}$, namely, $T_{\rm s} = 0.05$ sec/step and $T_{\rm s} = 0.25$ sec/step. All simulations are run for 400 sec and the RMS for the last 100 sec is computed. For these values, each period of the uncontrolled mode corresponds to approximately 20 samples and 4 samples, respectively. In both cases, the sample interval is less than the largest sample interval that avoids aliasing of the uncontrolled lightly damped mode, namely, $T_{\rm s} = 0.5$ sec/step, which corresponds to approximately 2 samples during each period of the uncontrolled mode. Using LQG with an internal model, the disturbance rejection performance is improved relative to LQG without an internal model. This improvement is more pronounced when the estimate of the peak-amplification frequency is close to the true peak-amplification frequency.

On the other hand, in Figure 3(c), LQG is applied to (51), with and without an internal model, using sampled-data control with $T_{\rm s} = 5$ sec/step. In this case, the lightly damped mode is undersampled, with 1 sample for approximately 5 cycles of the uncontrolled mode. Consequently, poor disturbance rejection performance is observed.

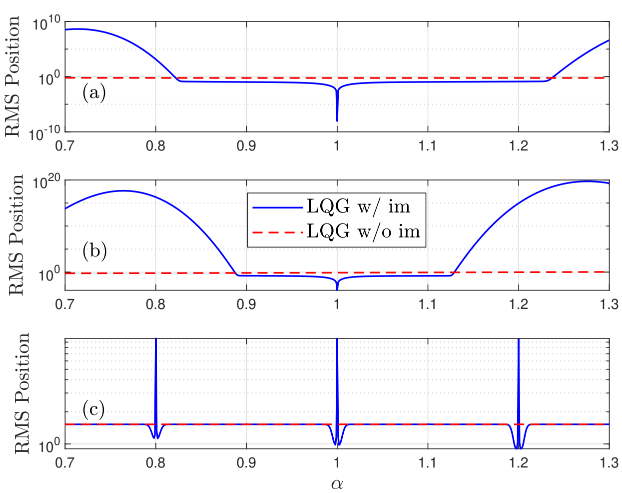

Fig. 3: RMS position of the lightly damped mode as a function of model uncertainty with and without an internal model (im) of the harmonic disturbance with sample interval (a) $T_{\rm s} = 0.05$ sec/step, (b) $T_{\rm s} = 0.25$ sec/step, and (c) $T_{\rm s} = 5$ sec/step. The parameter α denotes the estimate $\alpha\omega_{\rm p}$ of the peak-amplification frequency $\omega_{\rm p}$ of the system used for constructing the internal model and for LQG synthesis. For $\alpha = 1$, the internal model captures the true harmonic disturbance frequency, and the model used by LQG is exact; all other values of α correspond to modeling error in the construction of the internal model as well as in the plant model used for LQG synthesis. For 600 values of α and for both types of controllers, the plot shows the RMS values of the position under a harmonic disturbance at the resonance frequency, that is, $\omega_{\rm dist} = \omega_{\rm p}$. Note that the sample intervals $T_{\rm s} = 0.05$ sec/step and $T_{\rm s} = 0.25$ sec/step are 10% of and 50%, respectively, of the largest sample interval that avoids aliasing of the uncontrolled lightly damped mode, whereas the sample interval $T_{\rm s} = 5.0$ sec/step is 10 times the largest sample interval that avoids aliasing of the uncontrolled lightly damped mode, in which case the lightly damped mode is severely undersampled.

B. PCAC-based disturbance rejection

PCAC is applied with $\ell = 50$, $\hat{n} = 20$, $Q = 1000 I_{50}$, $R = 0.0001$, $\eta = 0.1$, $\tau_{\rm n} = 40$, $\tau_{\rm d} = 200$, $\Delta U_{\max} = -\Delta U_{\min} = 5$, $U_{\max} = -U_{\min} = 10$, $P_0 = I_{40\times 40}$, and the uninformative model $\theta_0 = 1\mathrm{e}{-10}\ \mathbf{1}_{40\times 1}$. The resulting RMS position is shown in Figure 4 for values of $T_{\rm s}$ between 0.01 and 5 sec/step. In all cases, PCAC has no prior knowledge of the system dynamics. Plots of the position versus time for sample intervals 0.05, 0.25, and 5 sec/step are shown in Figure 5. The model identified by PCAC for $T_{\rm s} = 0.25$ sec/step is shown in Figure 6. The disturbance frequency corresponds to a pole on the unit circle at $\pi/2$. The zero at $\pi/2$ and the nearby pole in the imaginary axis approximately capture the disturbance. This feature allows PCAC to use the identified model to predict the frequency, amplitude, and phase of the harmonic response for use in receding horizon optimization. For details, see [16].

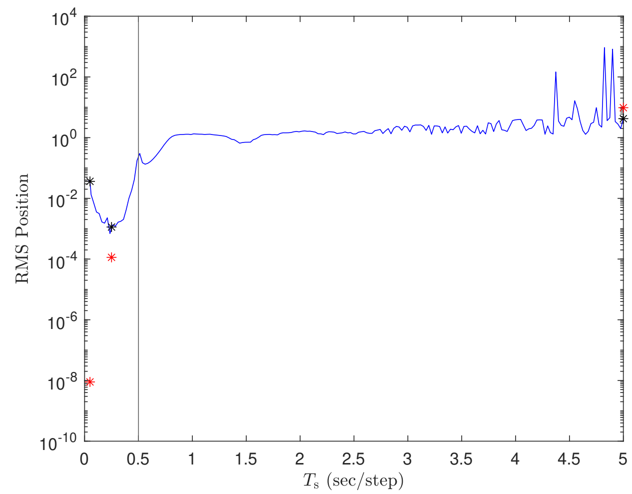

Fig. 4: RMS position versus sample rate of the PCAC controller for the lightly damped system with a rigid body mode. The vertical line corresponds to the largest sample interval that avoids aliasing of the uncontrolled lightly damped mode. The black and red stars correspond to the responses of PCAC and LQG with and internal model, respectively, for the sample intervals 0.05, 0.25, and 5 sec/step.

VI. Conclusions

Lightly damped modes that lie either inside or outside the bandwidth of an attitude control system present a longstanding challenge. This paper considered the case where the lightly damped mode is unmodeled, possibly severely undersampled, and excited at the modal frequency by a harmonic disturbance, that is, resonance. Sampled-data LQG control, which requires a model of the system dynamics, was applied to this problem to provide a performance baseline. To address the situation where the lightly damped mode is unmodeled, predictive cost adaptive control (PCAC), an indirect adaptive control extension of model predictive control, was applied. With no prior modeling information, PCAC performs concurrent online system identification to construct a model that captures the unknown system dynamics including a model of the harmonic disturbance that predicts

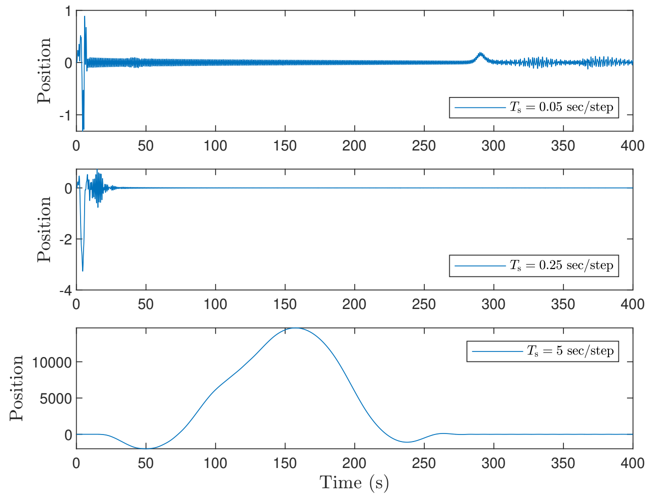

Fig. 5: Position versus time for sample intervals of 0.05. 0.25, and 5 sec/step, which were considered for LQG in Figure 3. PCAC stabilizes the response in all cases.

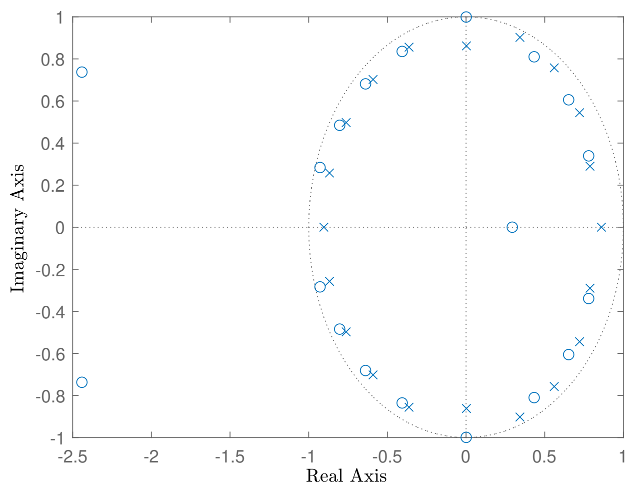

Fig. 6: Model identified by PCAC for $T_s = 0.25$ sec/step. The disturbance frequency corresponds to a pole on the unit circle at $\pi/2$. The zero at $\pi/2$ and the nearby pole on the imaginary axis approximately capture the disturbance for predicting the future response of the system.

the frequency, amplitude, and phase of the future response. Numerical results show that PCAC is effective in suppressing the lightly damped mode for sample intervals that are both smaller and larger than the largest sample interval that avoids aliasing.

VII. Acknowledgment

The authors thank Pete Washabaugh for helpful discussions.

References

[1] J. Vaughan, A. Yano, and W. Singhose, "Comparison of Robust Input Shapers," *Journal of Sound and Vibration*, vol. 315, no. 4, pp. 797–815, 2008.

[2] D. F. Enns, "Rocket Stabilization as a Structured Singular Value Synthesis Design Example," *IEEE Contr. Sys. Mag.*, vol. 11, no. 4, pp. 67–73, June 1991.

[3] C. Fuller and A. von Flotow, "Active control of sound and vibration," *IEEE Contr. Sys. Mag.*, vol. 15, no. 6, pp. 9–19, 1995.

[4] C. R. Fuller, S. J. Elliott, and P. A. Nelson, *Active Control of Vibration*. Academic Press, 1996.

[5] A. Preumont, *Vibration Control of Active Structures: An Introduction*, 4th ed. Springer, 2018.

[6] S. M. Kuo and D. R. Morgan, *Active Noise Control Systems: Algorithms and DSP Implementations*. Wiley, 1995.

[7] L. Sievers, G. Blackwood, M. Mercadal, and A. von Flotow, "MIMO Narrowband Disturbance Rejection using Frequency Shaping of Cost Functionals," in *Proc. Amer. Contr. Conf.*, 1991, pp. 1353–1359.

[8] L. Sievers and A. von Flotow, "Comparison of two lqg-based methods for disturbance rejection," in *Proc. IEEE Conf. Dec. Contr.,*, 1989, pp. 483–485.

[9] B. Francis and W. Wonham, "The Internal Model Principle of Control Theory," *Automatica*, no. 5, pp. 457–465, 1976.

[10] J. B. Hoagg, M. A. Santillo, and D. S. Bernstein, "Internal Model Control in the Shift and Delta Domains," *IEEE Trans. Autom. Contr.*, vol. 53, pp. 1066–1072, 2008.

[11] C. Rohrs, L. Valavani, M. Athans, and G. Stein, "Robustness of continuous-time adaptive control algorithms in the presence of unmodeled dynamics," *IEEE Trans. Autom. Contr.*, vol. 30, pp. 881–889, 1985.

[12] T. Nguyen, S. A. U. Islam, D. S. Bernstein, and I. Kolmanovsky, "Predictive Cost Adaptive Control: A Numerical Investigation of Persistency, Consistency, and Exigency," *IEEE Contr. Sys. Mag.*, vol. 41, pp. 64–96, Dec. 2021.

[13] J. B. Rawlings, D. Q. Mayne, and M. M. Diehl, *Model Predictive Control: Theory, Computation, and Design*, 2nd ed. Nob Hill, 2017.

[14] S. V. Raković and W. S. Levine, *Handbook of Model Predictive Control*. Birkhäuser, 2019.

[15] G. Takacs and B. Roha-Ilkiv, *Model Predictive Vibration Control: Efficient Constrained MPC Vibration Control for Lightly Damped Mechanical Structures*. Springer, 2012.

[16] S. A. U. Islam, K. Aljanaideh, T. W. Nguyen, I. V. Kolmanovsky, and D. S. Bernstein, "The Free Response of an Identified Model of a Linear System with a Completely Unknown Harmonic Disturbance Exactly Forecasts the Free-Plus-Forced Response of the True System Thereby Enabling Adaptive MPC for Harmonic Disturbance Rejection," in *Proc. IEEE Conf. Dec. Contr.*, Dec. 2021, pp. 3036–3041.

[17] N. Mohseni, T. W. Nguyen, S. A. U. Islam, I. V. Kolmanovsky, and D. S. Bernstein, "Active Noise Control for Harmonic and Broadband Disturbances Using RLS-Based Model Predictive Control," in *Proc. Amer. Contr. Conf.*, July 2020, pp. 1393–1398.

[18] N. Mohseni and D. S. Bernstein, "Predictive Cost Adaptive Control of Flexible Structures with Harmonic and Broadband Disturbances," in *Proc. Amer. Contr. Conf.*, June 2022, pp. 3198–3203.

[19] B. Wie and D. S. Bernstein, "Benchmark Problems for Robust Control Design," *AIAA J. Guid. Contr. Dyn.*, vol. 15, pp. 1057–1059, 1992.

[20] R. Stengel, *Stochastic Optimal Control: Theory and Application*. Wiley, 1986.

[21] A. L. Bruce, A. Goel, and D. S. Bernstein, "Convergence and consistency of recursive least squares with variable-rate forgetting," *Automatica*, vol. 119, p. 109052, 2020.

[22] N. Mohseni and D. S. Bernstein, "Recursive least squares with variable-rate forgetting based on the f-test," in *Proc. Amer. Contr. Conf.*, 2022, pp. 3937–3942.

[23] J. J. McKeon, "F approximations to the distribution of Hotelling's T_0^2," *Biometrika*, vol. 61, no. 2, pp. 381–383, 08 1974.

[24] D. Inman, *Engineering Vibration*, 5th ed. Pearson, 2021.